

Synthesis of Molecular Magnets

Mario Ruben

Institute of Nanotechnology, Research Centre Karlsruhe, Germany
Mario.Ruben@int.fzk.de

Content

1. Introduction

2. Molecular Organic Magnets

3. Molecular Inorganic Organic Magnets

3.1. Infinite 1D-, 2D-, 3D-, Networks: Molecular Magnetic Solids

3.2. Finite Cluster Compounds: Single Molecule Magnets (SMMs)

3.3. Infinite 1D-Coordination Polymers: Molecular Single Magnets (SCMs)

3.4. Molecular Magnetic Wheels

4. Spin Transition (ST) Compounds

5. Valence Tautomeric (VT) Compounds

6. References

1 Introduction

Molecular magnetism can be defined as the interdisciplinary area where the techniques of molecular chemistry are exploited in order to design and to synthesize new classes of magnetic materials, which are based on molecular lattices, rather than the continuous lattices of classical magnets. The molecular bricks have to bear unpaired electrons, which can be located either in s- or p-orbitals, as the case in pure organic magnets, or in d- or f-orbitals involving transition or lanthanide metal ions (Figure 1).

In comparison to nanoparticles of similar size, molecular compounds exhibit *a priori* high monodispersity in size, volume, shape and charge. Additionally, they are soluble in common solvents and the modular character opens ways to fine-tune their properties. With regard to the magnetic properties, such molecular systems exhibit features which might be considered both in classical (e.g. magnetic hysteresis, switching, exchange coupling) as well as in quantum (e.g. quantum tunnelling of magnetisation) regime.

The field of molecule based magnetism involves materials built-up from (i) pure organic bricks or (ii) from the combination of organic material and inorganic metal ions or clusters. The utilisation of metal ions has capitalized on the specific properties of structurally well-defined and versatile supramolecular materials.[1] Resulting supramolecular motifs are the one-, two- and three dimensional network architectures, self-assembled from (i) polyatomic, organic radical-bearing ligands and (ii) metallic centres that carry a magnetic moment.[2] By combination of organic synthesis with the supramolecular self-assembly approach, any deliberate arrangement of paramagnetic units in space is feasible within an extended network, from which the magnetic properties will result as consequence of specific short and long range ordering phenomena.

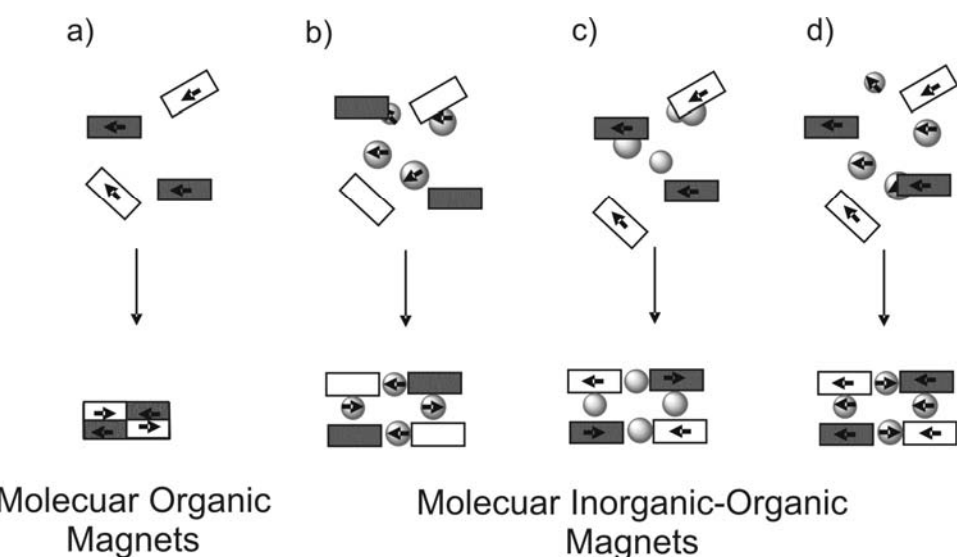


Fig. 1: Top: Schematic representation of the supramolecular approach to magnetic materials: Self-assembly of a) organic molecules (rectangles) or of b-d) organic molecules together with inorganic ions or clusters (spheres); the arrows mark the spin-bearing constituents, respectively.

2 Molecular Organic Magnets

Until the beginning of the 1990es, no genuine organic magnetic material only based on s- and p- electrons was known. The pioneering work of Itoh and Iwamura [3] showed for the first time that strong ferromagnetic coupling could be realised in polycarbene (Figure 2, top). The two unpaired electrons on each centre are in orthogonal orbitals, therefore they are in a $S = 1$ state. The disposition in *meta* around the aromatic rings results in quasi degenerate molecular orbitals, with strong ferromagnetic coupling.

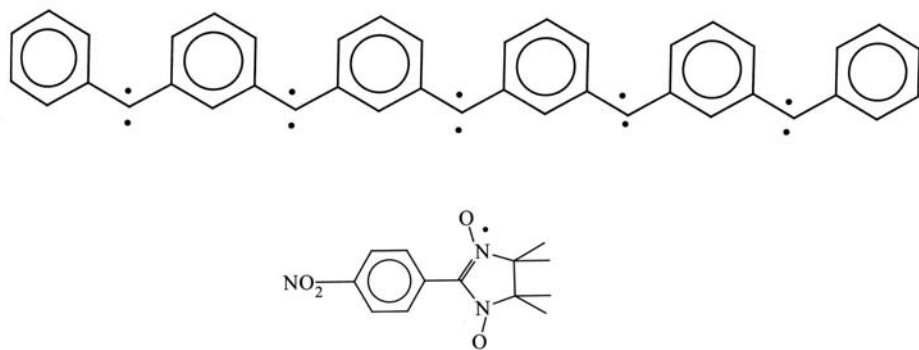


Fig. 2: Two examples of magnetic magnets showing magnetic ordering: polycarbene (top) and nitronyl nitroxide radicals (bottom)

In general, there are three conditions necessary to achieve a purely organic, preferably high, temperature magnet: (i) assemblage of organic-based unpaired electrons in high concentration; (ii) operation of strong exchange interactions aligning the spins; and (iii) formation of magnetic domains in which all the spins are ordered in extended networks in mesoscopic scale. However, the realization of necessarily strong exchange coupling between neighbouring organic molecules through van der Waals forces, Hydrogen bonds, hydrophobic interaction, etc. is expected to be difficult. Nevertheless, relatively strong ferromagnetic ordering was found for the class of organic nitronyl nitroxide radicals (Figure 2, bottom) with the highest reported ordering temperature of 1.4 K, so far. [4] The use of fullerenes raised the ordering temperature as expression of the coupling strength up to 16 K, [5] while eventually 36 K could be achieved by using sulphur nitrogen radicals. [6]

3 Molecular Inorganic-Organic Magnets

3.1. Infinite 1D-, 3D- and 2D-networks: Molecular Magnetic Solids

3.1.1. Oxalato-based 1D-, 2D-, and 3D-Magnets

One of the challenges in the field of supramolecular self-assembly of molecular inorganic-organic magnets is the controlled, spontaneous generation of well-defined architectures from both organic and inorganic building blocks (see Figure 1, b-d). A high structural organization can be ensured through the multiple one- to three-binding of transition metals giving rise to a variety of extended networks. The emphasis here lies in the design of the organic bricks (thereafter called ligands) together with the proper choice of the metal ions, since the overall topology of the network is strongly influenced by the match (or mismatch) of coordination algorithm of the linking metal ions with the binding properties (electronic, spatial, etc.) of the bridging ligands. Thus, the *bis*-chelating coordinating ability of ligands of the oxalate-type (Ox) has made them to a versatile choice for interconnecting different spin-bearing metal ions in extended networks (Figure 3, top). Indeed, the self-assembly of inorganic architectures incorporating bridging oxalato-type units have yielded various types of frameworks, which include 1D-chains, [7] 2D layers, [8] and 3D networks.[9]

Most of the so far investigated infinite chain-like compounds use the modified oxalato ligand $\text{Ox}-\text{CH}_2-\text{CH}_2-\text{CH}_2-\text{Ox}$ incorporating two interconnected oxalato-units and are of bimetallic character as shown for compound $[\text{Mn}^{\text{II}}(\text{Ox}-\text{CH}_2-\text{CH}_2-\text{CH}_2-\text{Ox})\text{Cu}^{\text{II}}(\text{Solvent})_x]_n$ in Figure 3, bottom. [10] The magnetic properties between 5 and 300 K can be interpreted as an antiferromagnetic coupling between the two neighbouring spins (here $S_{\text{Mn}} = 5/2$ and $S_{\text{Cu}} = 1/2$), while below 5 K magnetic AF ordering due to interchain exchange can be observed. [11] All investigated compounds of this type exhibit antiferromagnetic ordering at low temperatures with T_N between 1.8 and 5 K, only the compound $[\text{Mn}^{\text{II}}(\text{H}_2\text{O})_2(\text{Ox}-\text{CH}_2-\text{CH}_2-\text{CH}_2-\text{Ox})\text{Cu}^{\text{II}}(\text{H}_2\text{O})]_n$ incorporating an OH-substituted interconnecting linker exhibits ferrimagnetic ordering with $T_N = 4.6$ K. The occurrence of both anti- and ferrimagnetic ordering can be explained as a combination of intrachain and interchain ligand-mediated metal-metal exchange interactions. Additionally, some of these compounds behave as metamagnets, where a small applied magnetic field (between 1-2 kOe) induces a long-range ferromagnetic-like ordering by compensating the rather weak (antiferromagnetic) interaction between the 1D-chains. [12]

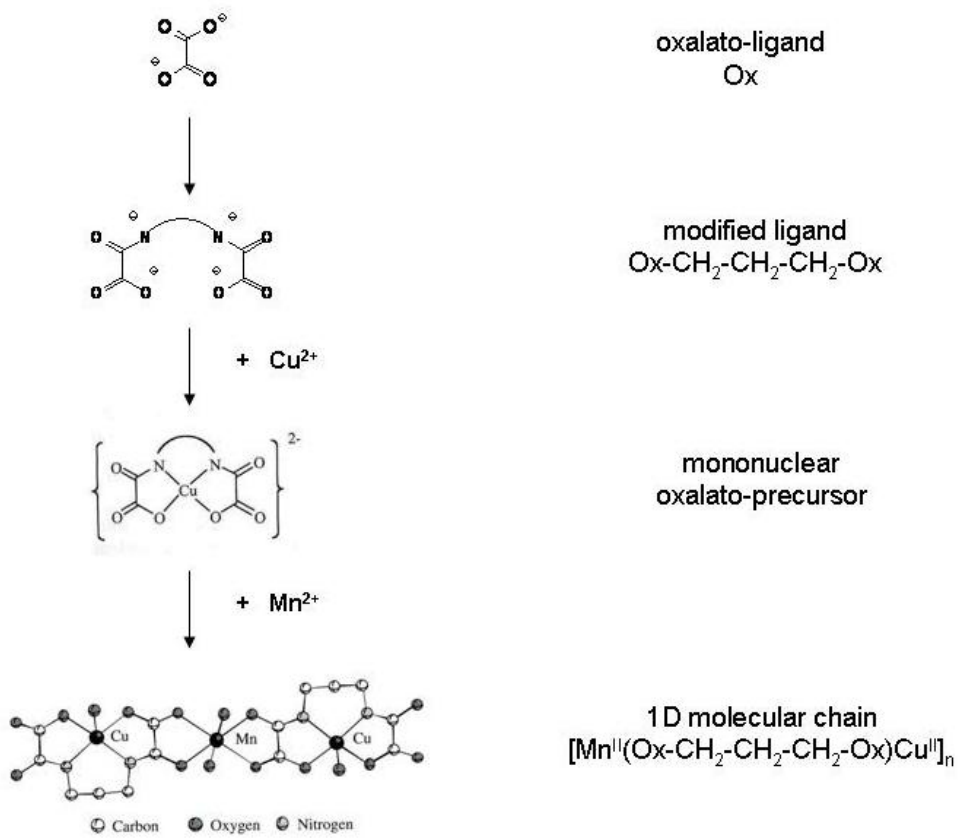


Fig. 3: Reaction scheme for the formation of the heterometallic oxalate-based 1D molecular compound $[\text{Mn}^{\text{II}}(\text{H}_2\text{O})_2(\text{Ox}-\text{CH}_2-\text{CH}_2-\text{CH}_2-\text{Ox})\text{Cu}^{\text{II}}(\text{H}_2\text{O})]_n \cdot 2\text{H}_2\text{O}$ exhibiting intrachain antiferromagnetic coupling. [10]

In order to increase the magnitude of the magnetic ordering, the Ox-ligands have been equally used in achieving 2D-spatial arrangement of spin-bearing metal-ions. Thus, the molecular building blocks $[\text{M}^{\text{II}}\text{M}^{\text{III}}(\text{Ox})_3]^{1-}$ and $[\text{M}^{\text{II}}(\text{Ox}-\text{CH}_2-\text{CH}_2-\text{CH}_2-\text{Ox})_3\text{Cu}^{\text{II}}_3]^{2-}$ (with M = transition or lanthanide metals) can be ordered in 2D sheet-like architectures, whereby the resulting negative charge of the resulting 2D-architecture is counterbalanced by positive cations A^+ .[13] [14] The nature of the electrostatically and interstitially bound cations A^+ determines, together with the chirality of coordinated metal centres, the overall structure by discriminating from other isoconstitutional and isostoichiometric 3D-networks. Thus, two dimeric units of alternating chirality are necessary to form a closed planar 2D structure with a hexagonal network motif.[15] The cations A^+ are mainly located between the anionic honeycomblayers and the systematic variation of A^+ can be used to modulate the separation between the layers and hence the interlayer magnetic exchange interaction.

Such Ox-based 2D polymeric materials exhibit a wide range of magnetic behaviour, and ferro, ferri or antiferromagnetic long-range ordering processes with critical temperatures ranging from 5-44 K, as well as short-range correlations and spin glass like behaviour have all been observed. Generally, the magnetic interactions and magnetic ordering in the $[\text{A}][\text{M}^{\text{II}}\text{M}^{\text{III}}(\text{Ox})_3]$ compounds is strongly dependant on the character of the cations A^+ as well as the combination of M^{II} and M^{III} metal ions.

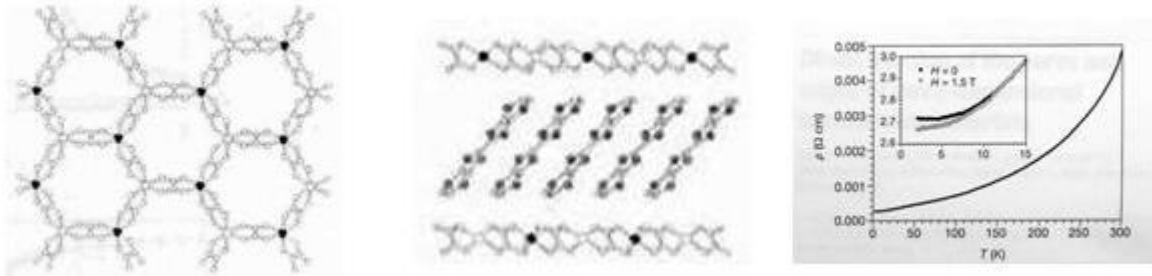


Fig. 4: Molecular structure of the hybrid material $[BEDT-TTF]_3[Mn^{II}Cr^{III}(Ox)_3]_n$: left) View of the oxolato-based bimetallic $[Mn^{II}Cr^{III}(Ox)_3]$ 2D honeycombe-like sublattice. middle) Representation of the alternation of the organic $[BEDT-TTF]$ - and of the inorganic $[Mn^{II}Cr^{III}(Ox)_3]^-$ layers. right) Thermal variation of the electrical resistivity with the inset showing the low-temperature magnetoresistance with the magnetic field applied perpendicular to the layers.[16]

The highlight of the anionic 2D-honeycomb-cation strategy was the realisation of the coexistence of ferromagnetism and metallic conductivity in the same material. The compound $[BEDT-TTF]_3[Mn^{II}Cr^{III}(Ox)_3]$ is built up from two molecular sublattices: a bimetallic 2D honeycomb network with ferromagnetically coupled metal ions ($T_c = 5.5$ K) and layered BEDT-TTF cations, which are intercalated between the oxalate layers and introduce electric conduction into the magnetic architecture (Figure 4). [16]

The self-assembly of Ox-bridged bimetallic units containing identical chiral information at both metallic centres results necessarily in the formation of 3D network structures. [15] The possibility of linking paramagnetic metal ions via Ox-bridges in 3D lattices opens interesting avenues to tailor-made functional materials. In recent years, the group of S. Decurtins reported on the structure of several anionic 3D networks based on the Ox-system $[M^I M^{III}(Ox)_3]^{2-}$ or $[M^{II}_2(Ox)_3]^{2-}$ ($M^{II/III}$ transition metals and $M^I = Li, Na$), where the cationic moiety A^+ consists in tris-chelated, transition metal imino complexes $[M^{II}(bpy)_3]^{2+}$ (with $M = Fe, Ru, Ni, Co$), which can be used as kind of “Trojan Horses” to introduce molecular functionalities into the material. All so far investigated compounds exhibit an analogously chiral anionic 3D (10,3) network, whereby the ten-gon framework demonstrates a marked structural flexibility towards the inclusion of the cations A^+ (Figure 5). [17] The robustness of the oxolato approach was also demonstrated by the isosteric replacement of the oxolato bridges by dithioxolato bridges ($C_2O_2S_2^{2-}$), what equally resulted in a topology, which is constituent to the chiral 3D (10,3) network. Finally, enantiomeric pure 3D network $[Cr^{III}(Ox)_3]^{3-}$ polymers could be obtained by the introduction of homochiral, that means enantiomeric resolved $[Ru^{II}(bpy)_3]^{2+}$ cationic A^+ building blocks. Such chiral materials may exhibit very interesting magneto-optical effect.[18]

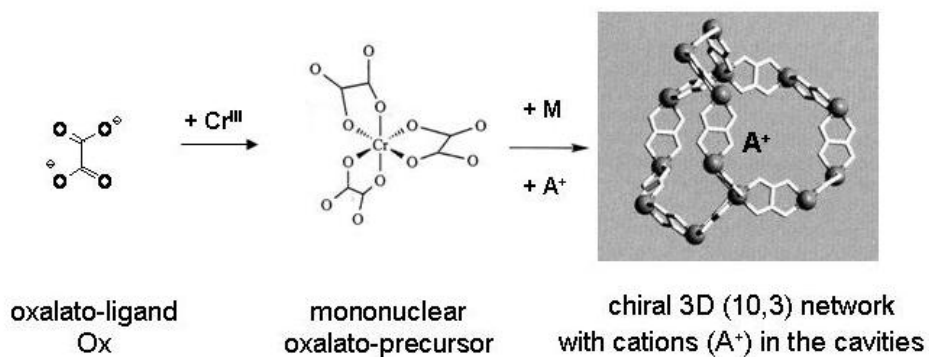


Fig. 5: Schematic representation of the stepwise formation of the bimetallic 3D anionic (10,3) network starting from the oxalate ligand. [15]

The 3D homo- and heterometallic oxalato bridged frameworks are examples of supramolecular compounds, which show long-range magnetic ordering. Additionally they possess the possibility to introduce further physical properties by the cations A^+ as guests within the internal cavities (Figure 5). Magnetic studies of the Ox-based 3D network $[Co^{III}(bpy)_3][Co^{II}_2(Ox)_3]ClO_4$ show the occurrence of a weak ferromagnetism at low temperatures ($T_c = 9.0$ K). This magnetic ordering is attributed to the spin canting of the magnetic moments in the chiral 3D oxalato-bridged cobalt (II) network and it was shown that the magnetic ordering strongly depends on the size and the magnetic character of the tris-chelated counterion. [19]

3.1.2. Cyano-based 3D-Magnets

The rational built-up approach of bimetallic polycyano compounds is based on (i) the linear bidentate binding mode of the cyan-bridging ligand (thereafter CN) and on (ii) the six-fold connectivity of the $B^{II}(CN)_6$ brick (B = first row transition metal), which together with octahedral coordinating metal ions A^{II} results in an overall neutral infinite cubic crystal lattice (Figure 6).

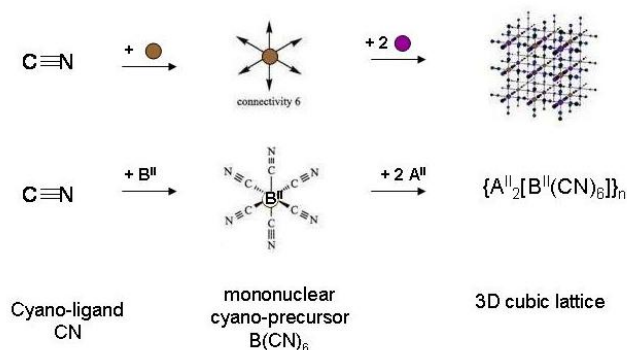


Fig. 6: Schematic representation of the self-assembly process of a infinite 3D cubic coordination network out of the CN ligand and two types of different metal ions B (brown) and A (violet).

The use of A^{III} metal ions leads to an (ideally) face-centred cubic negatively charged network structure $\{A^{III}_p[B^{II}(CN)_6]_q\}^{1-}$, in which the electroneutrality is kept by the introduction of monovalent alkali ions C¹⁺ (C= Na, K, Rb, Cs) at interstitial lattice positions. This simple and appealing cubic structure is well-known as the so-called “Prussian blue”-structure, but is also strongly reminiscent to the lattice structure of perovskites. Chemical synthesis can control the nature of the involved metal ions, but can also create sizable departures from the ideal stoichiometry with C⁺ vacancies or B(CN)₆ substitutions partially filled with solvent molecules. The very general cubic A-CN-B matrix offers a wide variety to develop the orbital interactions in the three directions of space by choosing very different paramagnetic anions A and B. The high symmetry of the system allows an efficient control of the nature and the amplitude of the magnetic exchange interactions between the metal ions.

It was very early shown that the original mixed valence Prussian-blue compound (A = Fe^{III} and B = Fe^{II}) shows a long-range ferromagnetic ordering at T_c = 5.6 K. [20] This is astonishing, since only the Fe^{III} sites carry a spin, whereas the Fe^{II} sites are diamagnetic and, consequently, the magnetic interactions must occur between the next-nearest ions through Fe^{III}-C-N-Fe^{II}—N-C-Fe^{III} linkages over a distance of 10.6 Å. This illustrates the possibility of propagating magnetic interactions through widely separated spin carriers in molecular compounds mainly due to the strong spin delocalization from the metal ions towards its nearest neighbours. The presence of strong spin densities on the nitrogen and carbon atoms of the cyano groups has been experimentally observed by polarized neutron diffraction.[21] Depending on the nature of A and B, one may obtain 3D anti- and ferromagnets or ferrimagnets. In Prussian-blue-like phases, the metal sites A and B are in octahedral surroundings, where the 3d valence orbitals are split into low-lying (*t*_{2g}) and high-lying (*e*_g) subsets. Since only the low-lying *t*_{2g} orbitals are occupied in B, the magnetism shown by the overall compound depends mainly by the nature of metal ion A.

If all unpaired electrons of A occupy *t*_{2g}-orbitals, the A-B interaction will be antiferromagnetic, and the compound will be a ferrimagnet based on the non-compensated spin moments. If the unpaired electrons of A occupy some *t*_{2g} orbitals and some *e*_g-orbitals, the A-B interaction will again be antiferromagnetic, but less pronounced than in the previous case, and the resulting compound will be a ferrimagnet, but with a lower critical temperature. Finally, if the unpaired electrons of A only occupy *e*_g-orbitals, the A-B interaction will be ferromagnetic, and the compound will be a ferromagnet.

Moving along this rationale, several molecular-based 3D solids with astonishing magnetic properties could be synthesized during the last decade. Thus, as a first highlight, the synthesis of the ferrimagnet Cr^{II}₃[Cr^{III}(CN)₆]₂.10 H₂O exhibiting a T_c of 230 K could be succeeded, which was followed by the synthesis of the compound V^{II}_{0.42}V^{III}_{0.58}[Cr^{III}(CN)₆]_{0.86}.2.8 H₂O being a room temperature molecular magnet with a T_c of 315 K. [22] [23] The V^{II} metal ions were partially oxidized to V^{III}, but since the magnetic orbitals of all involved metal ions (V^{II}, V^{III} and Cr^{III}) have the same symmetry and both V^{II}-Cr^{III} and V^{III}-Cr^{III} interactions are antiferrimagnetically, the overall magnetic coupling scheme results in a ferrimagnet with very high critical temperature.

However, the stoichiometric composition of the compound $V^{II}0.42V^{III}0.58[Cr^{III}(CN)_6]_{0.86} \cdot 2.8 H_2O$ points rather to an amorphous and non-stoichiometric extended solid than to a defined molecular compound. In this respect, this system resembles to the first, previously reported room temperature magnet synthesized from molecular precursors: Although its structure is still under discussion, the amorphous material of the composition $V^{II}(TCNE)_2 \cdot 1/2 (CH_2Cl_2)$ (TCNE being the radical anion of tetracyanoethylene) is even exhibiting an (estimated) T_c of 350 K.[24]

Furthermore, Hashimoto et al. observed interesting photo-induced magnetization phenomena in a powder sample of the stoichiometry of $K_{0.2}Co_{1.4}Fe(CN)_6 \cdot 6.9 H_2O$. Its magnetisation and T_c values are significantly increasing by red light illumination and the enhanced magnetization is partly reduced by blue light illumination. This photo effect is explained by the charge-transfer induced spin transition between $Fe^{II} (t_{2g}^6 e_g^0; S = 0)$ -CN-Co^{III}($t_{2g}^6 e_g^0; S = 0$) and $Fe^{III} (t_{2g}^5 e_g^0; S = 1/2)$ -CN-Co^{II}($t_{2g}^5 e_g^2; S = 3/2$) states by light irradiation. [25]

3.2. Finite Cluster Compounds: Single-Molecule Magnets (SMMs)

An exciting development in nanoscale magnetic materials occurred in 1993, when $[Mn_{12}O_{12}(O_2CMe)_16(H_2O)_4]$ (hereafter Mn₁₂) was identified as nanoscale magnet.[26] It was the first molecular compound, which comprised discrete, magnetically non-interacting molecular units rather than a 3D extended lattice (as in metals and metal oxides, for example). The discovery initiated the field of molecular nanomagnetism and such molecules have since been termed single-molecule magnets (SMMs). They derive their special magnetic properties from the combination of a large spin (S) and an Ising (easy-axis) magneto-anisotropy exhibiting a negative zero-field splitting parameter (D), which gives rise to the superparamagnetic-like property of a barrier to magnetization relaxation (Figure 7). This class of compounds does not only display magnetisation hysteresis, but also quantum tunnelling of magnetisation (QTM) [27] and quantum phase interference. [28]

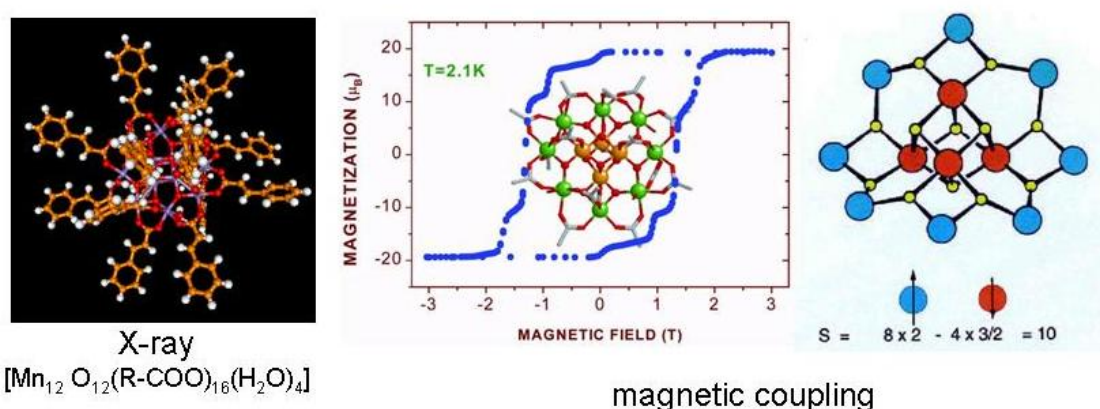


Fig. 7: Molecular structure (left), magnetic curve (middle), and magnetic coupling scheme (right) of the Mn₁₂ family exhibiting magnetic hysteresis and quantum tunnelling of magnetization (QTM).

Since the initial discovery of Mn_{12} molecule, a number of other types of molecules have been discovered, almost all of them being transition metal clusters, and the majority of those Mn-oxo clusters containing 2-84 Mn^{II}, Mn^{III} and Mn^{IV} ions, a multitude of oxo bridges (M-O-M), and several peripheric organic, mostly carboxylate, ligands. [29] So far, the synthetic efforts directed towards new compounds of this particular type were guided along two along two main guides: (i) to control the nuclearity of the cluster systems and (ii) to increase the anisotropy barrier height of the intrinsic magnetism. The combined synthetic and magnetic efforts of mainly Wernsdorfer and Christou et. al. yielded in a large variety of Mn_x-cluster SMMs exhibiting spherical, disk-like, ring-like, or even rod-like morphologies and topologies (Figure 8). [30]

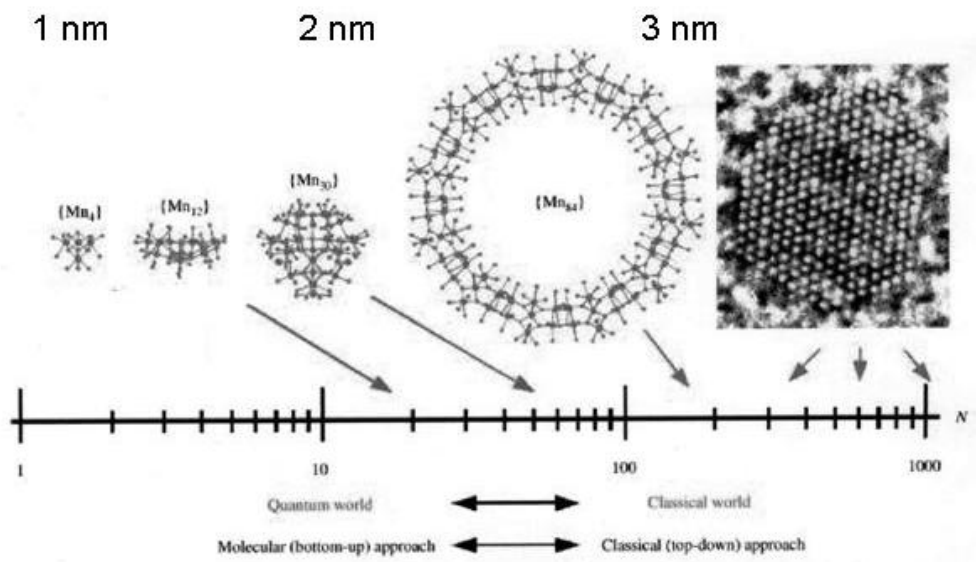


Fig. 8: Several examples of Manganese-Oxo-cluster SMMs depicted together with their size (top) and Néel-vektor (bottom) and in comparison to superparamagnetic nanoparticles (right). (taken from [29]).

A further group of SMMs investigated during the last years is the $\text{Mn}_4\text{O}_3\text{X}$ family, in which the manganese ions are exhibiting a distorted-cubane core of virtual C_{3v} symmetry. The metal centres are mixed valence exhibiting frequently three Mn^{III} and one Mn^{IV}, which are coupled by μ_3 -O-bridges to a well isolated ground state spin of $S = 9/2$.[31] Some of these complexes crystallize as head-to head dimmers, which have allowed for the first time the identification of exchange-biased quantum tunnelling of magnetization (QTM) [32] and of quantum coherence in SMMs. [33]

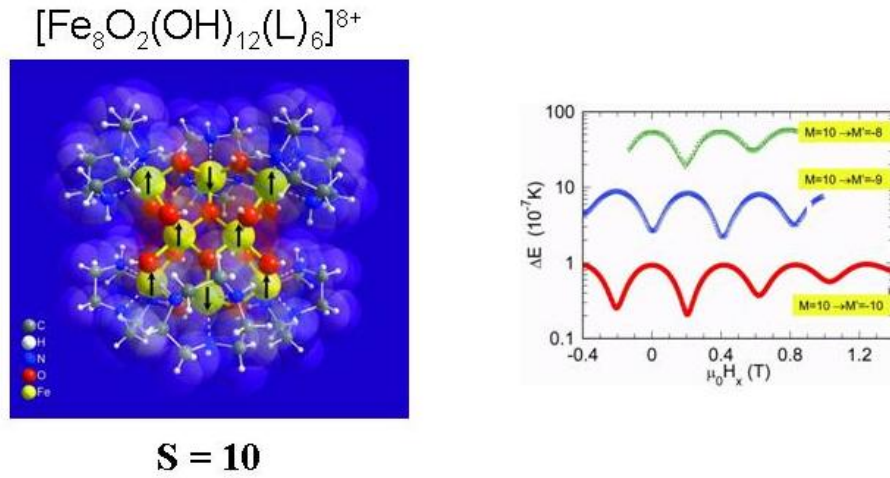


Fig. 9: Molecular Structure of $[\{\text{Fe}^{\text{III}}_8\text{O}_2(\text{OH})_{12}(\text{L})_6\}\text{Br}_7\text{H}_2\text{O}]\text{Br}.8\text{H}_2\text{O}$ (L = organic ligand) and field dependence of the tunnel splitting when the field is applied along the hard axis. [34]

Recently, tetranuclear Fe^{II}_4 cubane-like and nononuclear Fe^{II}_9 complexes were synthesized and have shown moderate magnetic anisotropy. [35][36] One of most intensely studied SMMs represents the molecule $[\{\text{Fe}^{\text{III}}_8\text{O}_2(\text{OH})_{12}(\text{L})_6\}\text{Br}_7\text{H}_2\text{O}]\text{Br}.8\text{H}_2\text{O}$ (L = organic ligand), [37] in which oscillation of the quantum tunnel splitting could be observed for the first time (Figure 9). [34] In addition, several extended $\text{Fe}^{\text{III}}_{19}$ oxo-cluster were prepared exhibiting SMM behaviour with modest barrier heights.[38] Finally, various SMMs incorporating different types of transition metals of various nuclearity M_x (with $M = \text{V}^{\text{III}}$ [39], Co^{II} [40], Ni^{II} [41]), including mixed-metal systems, [42] have been prepared with S values ranging with 3 to 13.

3.3. Infinite 1D Complexes: Molecular Single Chain Magnets (SCM's)

Taking into account the above described characteristics of SMMs (high spin ground state S , negative zero field splitting parameter D with resulting magnetic anisotropy axis), one idea would be to go one step further towards extended 1D restricted molecular systems and to synthesize magnetically active infinite coordination polymers, which have been named “single chain magnets” (SCM). To design this type of system, three essential ingredients need to be considered: (i) spin carriers must exhibit a strong uniaxial anisotropy to be able to block or to “freeze” their magnetization in one direction. (ii) The material needs to exhibit a spontaneous magnetization to be called a magnet, whereby the individual magnetic moments in the chain must not cancel out in the “frozen” state. (iii) The chains must be isolated magnetically as much as possible to avoid 3D ordering. The occurrence of slow relaxation and Arrhenius behaviour of the relaxation time in such systems was already predicted theoretically by Glauber using a 1D Ising model in the 1960ies. [43]

On the base of Glauber's prediction, helical Co^{II}-nitronyl nitroxide chains $[[\text{Co}^{\text{II}}(\text{hfac})_2(\text{NITPhOMe})]$; Figure 10) acting as molecular magnetic wires were first synthesized and investigated by Gatteschi et. al. in 2001. [44] The molecular chains behave as 1D ferrimagnets, because of the non-compensation of the magnetic moments of the Co^{II} and the organic radical centres. The susceptibility below 50 K is strongly anisotropic with an easy axis of magnetization and the relaxation time of the magnetization shows strong frequency dependence in ac susceptibility measurements. This seems to be physically reasonable, since the Glauber model for Ising ferromagnetic chains predicts that the reversal of the spins becomes more difficult at low on lowering the temperature because the short-range correlation along the chains favours the parallel alignment of the spins. Consequently, an Arrhenius behaviour is predicted for the relaxation time, with the height of the barrier corresponding to the nearest-neighbour exchange interaction. [45]

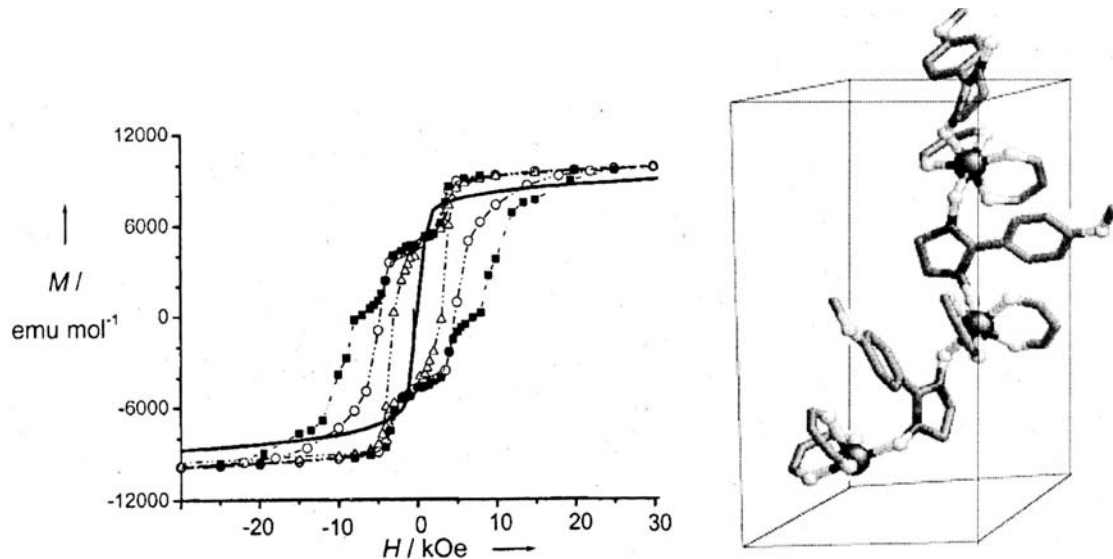


Fig. 10: Molecular structure of the helical Co^{II}-nitronyl nitroxide chain $[[\text{Co}^{\text{II}}(\text{hfac})_2(\text{NITPhOMe})]$ and hysteresis loops observed on a single crystal by applying magnetic fields parallel to the chain axis at 2.0 K (squares), 3.0 K (circles), 4.5 K (triangles), and at 2.0 K parallel to it (line). [44]

Recently, the synthesis and magnetic investigation of two further, now mixed-metal, 1D molecular chains, $\{[\text{Fe}^{\text{III}}(\text{L})(\text{CN})_4]_2\text{Co}^{\text{II}}(\text{H}_2\text{O})_2\} \cdot 4\text{H}_2\text{O}$ and $[\text{Mn}_2(\text{L}^1)_2\text{Ni}(\text{L}^2)(\text{Py})_2](\text{ClO}_4)_2$, confirmed the general validity of the Glauber approach in respect to Single Chain Magnets.[45][46] Interestingly, however, other 1D systems containing Mn^{II} and Mn^{III} metal ions did not express the equivalent magnetic behaviour.[47] [48]

3.4. Magnetic Molecular Wheels

Molecular wheels are excelled by a virtually perfect ring-like arrangement of the metal ions within a single molecule. The decanuclear wheel $[\text{Fe}^{\text{III}}_{10}(\text{OCH}_3)_{20}(\text{O}_2\text{CCH}_2\text{Cl})_{10}]$, generally called Fe_{10} , has become the prototype for this class of compounds.[49] In the last decade, various wheels with different metal ions and number of centres were realized, whereby a difficult to rationalize preference of even-numbered wheels has been manifested. [50]

In view of their structure, antiferro- or ferromagnetically coupled wheels are widely regarded as finite equivalents for infinite magnetic 1D chains (*vide infra*), implying that physical concepts found for these chains should describe them, too. Even-numbered, AF-coupled wheels are characterized by an $S=0$ spin ground state, which makes them unsuitable as a SMMs. However, excited magnetic states seem to be easily accessible and first insight into the higher lying magnetic spectrum was given by the observation of steps in magnetization and torque measurements at very low temperatures.[51] Additionally, the molecular wheels were proposed to be able to show large quantum effects, such as tunnelling of the Néel vector [52] or quantum coherence phenomena.[53] Furthermore, very similar wheels systems form a suitable series of objects to investigate the origins of magnetic anisotropy, partly because of their high symmetry, which was investigated in closer detail in different Co^{II}_4 and Cr^{III}_8 systems. [54] [55]

Magnetic studies of the Co^{II}_4 systems as function of temperature revealed intramolecular antiferromagnetic exchange interactions.[56] Subsequently recorded magnetisation curves on single crystals of certain Co^{II}_4 - rings at 1.9 K unravelled following anisotropic situation: For magnetic fields perpendicular to the grid plane, the magnetization shows a behaviour reminiscent of a thermally broadened magnetization step due to a ground-state level crossing, as it is often observed in antiferromagnetic clusters.[57] In contrast, the magnetic moments for applied fields within the plane of the Co^{II}_4 -wheel, increase linearly with equal slope as function of the magnetic field (Figure 11). No longe-range ordering develops as intermolecular interactions are negligibly small preventing the system from undergoing a metamagnetic phase transition. However, the analysis of its magnetism can be completely recast in the language of metamagnetism, and in this sense it was proposed to call them single-molecule metamagnets. [58]

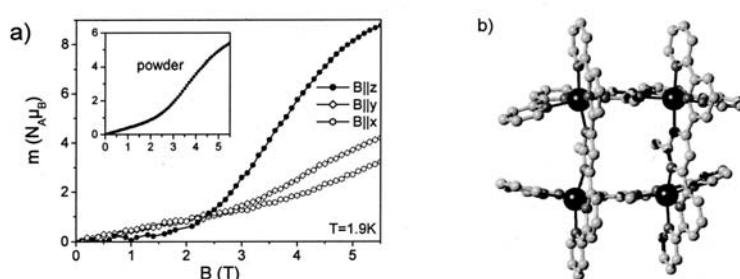


Fig. 11: Molecular structure Co^{II}_4 wheels (right) and the field dependence of the magnetic moment of a single crystal at 1.9 K for magnetic fields along the main axes (left). The inset displays the magnetization curve of the powder sample. [58]

Approaches to remove the diamagnetic S=0 ground state consist in either (i) the introduction of hetero-metal ion into the ring or (ii) the synthesis of odd-numbered rings. Both routes will lead to wheels, in which magnetic frustration rules. Examples proving the feasibility of both routes could be realized recently: Following the protocol of a formerly described Cr^{III}₈ wheel, a series of hetero-metal ion wheels of the composition Cr^{III}₇M (with M = Ni^{II}, Co^{II}, Mn^{II}, and the diamagnetic Cd^{II}) and Cr^{III}M₂ (with M = V=O) could be obtained. [59] First magnetic investigations have proven, that the Cr^{III}₇M wheels act, as expected, as antiferromagnetically coupled wheels with a nondiamagnetic ground state at low temperature.

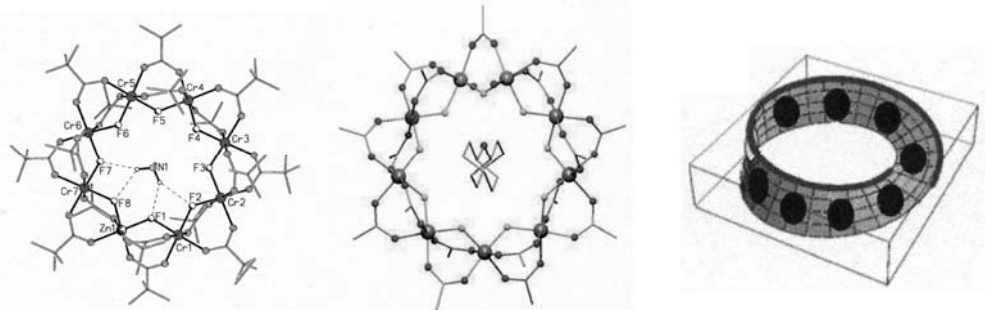


Fig. 12: Schematic molecular structures of the heterometallic even-numbered Cr^{III}₇Zn^{II} wheel (left), and the hetero-metallic odd-numbered Cr^{III}₈Ni^{II} wheel (middle). The visualisation of the Möbius-strip type “magnetic knot” delocalized on the Cr^{III}₈ chain (black circles, white circle: Ni^{II}) within the latter one. [60]

Using the same synthetic procedure, odd-numbered Cr^{III}₈Ni^{II}, Cr^{III}₈Co^{II} and Cr^{III}₇(V=O)₂ were accessible, too. The magnetic behaviour of these nonanuclear wheels is deserves some special attention: The Cr^{III}₈Ni^{II} compound contains an even number of unpaired electrons due to the presence of a Ni^{II} ion, with S = 1, and eight Cr^{III} ions with S = 3/2 spins; this would even allow a diamagnetic ground state. Nevertheless, not all the antiferromagnetic interactions can be simultaneously satisfied in the Cr^{III}₈Ni^{II} wheel and therefore the magnetic situation has to be regarded as frustrated. A way to visualize this problem is its analogy with the Möbius strip having a “magnetic knot”, which represents within the wheel the point of spin frustration (where neighboured spins can not align in antiparallel fashion). Detailed magnetic investigations could determine the place of the “magnetic knot” delocalized within the Cr^{III}₈ chain, and not as expected at the single Ni^{II} ion (Figure 12). [60]

4 Spin Transition (ST) Compounds

As a consequence of the splitting of the energy of the d-orbitals into t_{2g} and e_g sets in a octahedral ligand field, complexes of certain transition metal ions, particularly those of the first transition series with configurations d^4 to d^7 , may exist in either high-spin (HS) or low-spin (LS) state. In weak ligand fields the ground state is HS exhibiting a spin multiplicity at its maximum, whereas strong ligand fields stabilize the LS state with a minimum multiplicity. For intermediate fields, the energy difference (ΔE^o_{HL}) between the lowest vibronic levels of the potential wells of two states may be sufficiently small, such application of some relatively minor external perturbation effects a change in the state. This phenomenon is known as a spin transition (ST) and it might be induced thermally if $\Delta E^o_{HL} = k_B T$, but also pressure-, light-, and soft x-ray induced spin transition phenomena have been observed. [61] [62] [63]

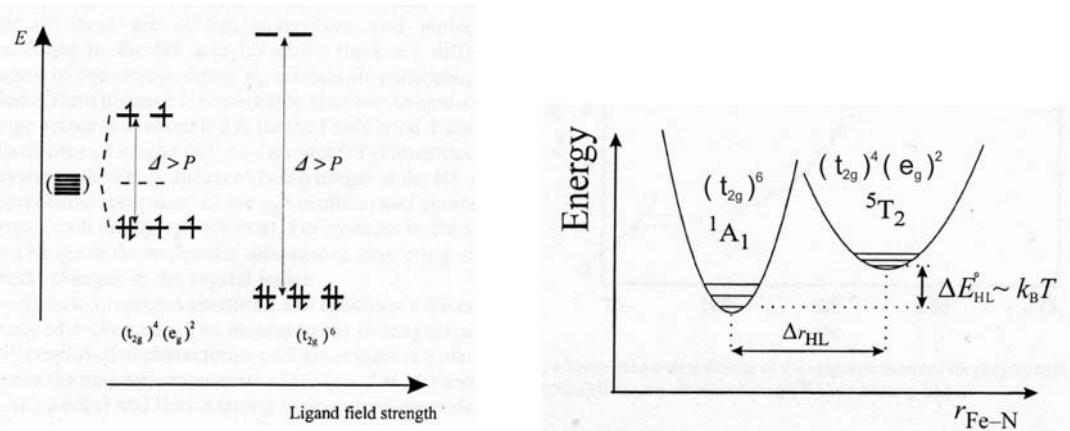


Fig. 13: left) Representation of the possible electronic configurations of a d^6 system in an octahedral ligand field (Δ : ligand field parameter; P : spin pairing energy). right) The resulting potential wells for the diamagnetic 1A_1 and the paramagnetic 5T_2 states (of octahedral Fe^{II}), the nuclear coordinate being the metal-donor atom distance. [64]

Although spin transitions have been observed for all the above mentioned electron configurations of the first transition series, by far the greatest number of research work deals with Fe^{II} and, to a lesser extend, with Co^{II} complexes. Especially, ST- Fe^{II} compounds are magnetically an appealing research object, since the spin transition occurs between the diamagnetic 1A_1 (LS) and the paramagnetic 5T_2 (HS) states (Figure 13), which can be easily followed by magnetic measurement techniques.

The driving force for thermally induced spin transition constitutes the considerable entropy gain ($50\text{-}80 \text{ J mol}^{-1} \text{ K}^{-1}$ for Fe^{II}) for the LS to HS conversion, made up of a magnetic component ΔS_{Mag} and a much greater vibronic entropy contribution ΔS_{Vib} arising from the higher degeneracies (degrees of freedom) in the HS state. The enthalpy change associated with the LS to HS conversion is typically in the range $6\text{-}15 \text{ kJ mol}^{-1}$ (for Fe^{II}) and is primarily due to the rearrangement of the coordination sphere (e.g. metal donor atom bond length increase). [65] In the solid state, an electron–phonon coupling enables the molecules within the lattice to communicate the spin state change. It is proposed that a local entropy driven spin state change, which is accompanied with a large change in the metal-donor atom bond distance (e.g. 0.2 \AA for $\text{Fe}^{\text{II}}\text{-N}$), creates a “point defect”, which is communicated to the surroundings resulting in a cooperatively concerted spin state change through the solid bulk. [66]

It is possible to evaluate the relative concentrations of HS and LS states in function of temperature from the measurement of the temperature-dependence of the magnetization. Regarding the plot of the HS molar fraction γ_{HS} vs. T , different forms of transition and different degrees of cooperativity can be found (Figure 14 a-e). The spin transition might be gradual and continuous over an extended temperature range as found in solutions, or it may be abrupt and occur within a narrow temperature range. The spin transition might be associated with a thermal hysteresis loop, or be a multi step process. In certain cases the spin transition might be incomplete at one or both extremes of the curve. The curves are diagnostic of the nature of the ST and the steepness of change is indicative, at least in solid state, of the extent of cooperativity involved into the propagation of spin change throughout the crystal lattice. A transition temperature is defined as that temperature at which fractions of HS and LS species, which take part in transition, are equal.

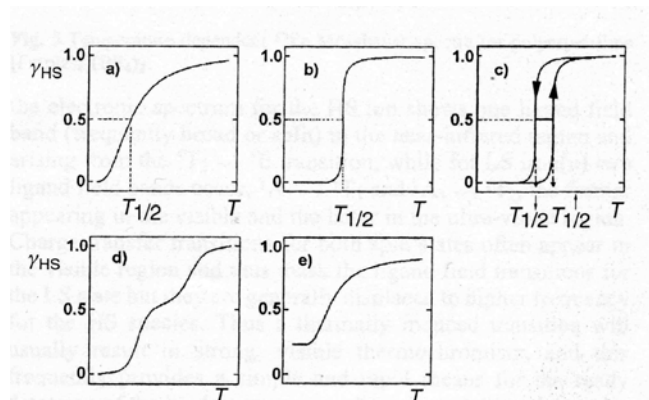


Fig. 14: The nature of ST curves; a) gradual; b) abrupt; c) with hysteresis; d) with steps; e) incomplete. [64]

By far most of the complexes exhibiting ST (>150) are mono-nuclear Fe^{II} compounds, where the metal ion is surrounded by a set of six N-donor atoms. The donor atoms are mainly part of a heterocyclic ring system, which can be arranged around the metal ion. The chemical nature of the ligands allows fine-tuning of the ligand field strength by (i) introduction of sterically crowding substituents close to the donor atoms; (ii) by changing the ring size from six to five membered rings, what reduces both the σ - and the π -acceptor strength of the ligands, and (iii) selective replacement of N-donor-atoms by less strongly coordinating O- or S- donor atoms. The first synthetic system, $[\text{Fe}(\text{phen})_2(\text{NCS})_2]$ (phen = 1,10 phenanthroline) was synthesized in 1966 and since then many other compounds of similar composition have been shown to undergo transitions (one typical example of a mononuclear ST- Fe^{II} -complex shown in Figure 15). [67]

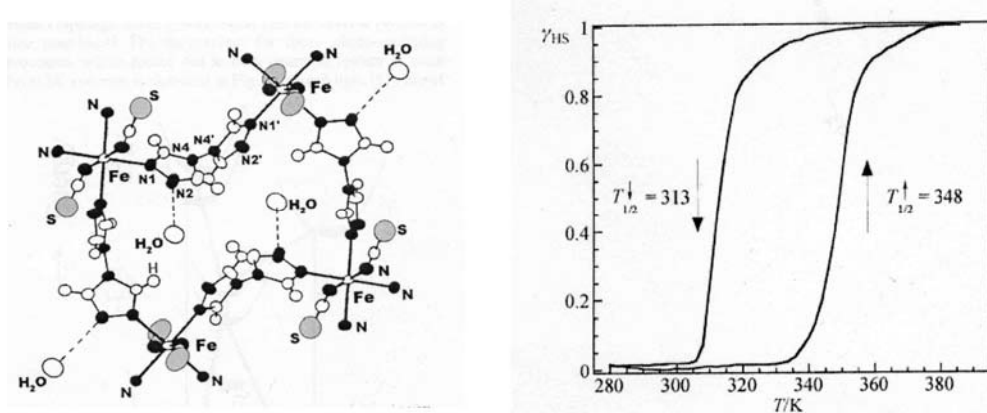


Fig. 15: Molecular structure (left) and temperature-dependence of the HS molar fraction (right) of the mononuclear spin transition complex $[\text{Fe}(\text{NH}_2\text{trz})_2](\text{NO}_3)_2$. [68]

Recently, several binuclear ST- Fe^{II}_2 complexes and even a binuclear ST- Co^{II}_2 were synthesized. [68] [69] Furthermore, a series of tetranuclear ST- Fe^{II}_4 -complexes was reported as so far largest oligomeric molecular ST architectures. [70] Interestingly, in both di- and tetranuclear species, covalently linking of Fe^{II} spin transition centres leads to very broad and gradual transitions without any hysteresis phenomena. This particular behaviour is assigned to the presence of a statistic distribution [HS-HS], [HS-LS], and [LS-LS] couples, which can be, at least in the case of [HS-HS], magnetically coupled and changing the magnetic situation within the respective molecule drastically. [71]

In continuation, such tetranuclear ST- Fe^{II}_4 units were used a functional bricks in the construction of extended 1D and 2D nano-architectures. Thereby, the transition temperature of 1D- columnar structure experienced a shift of ca. 200 K towards higher temperatures (compared to the unconnected ST- Fe^{II}_4 brick), while the 2D structure frozen in its LS state as consequence of the increased molecular rigidity in the extended 2D architectures (Figure 16). [72]

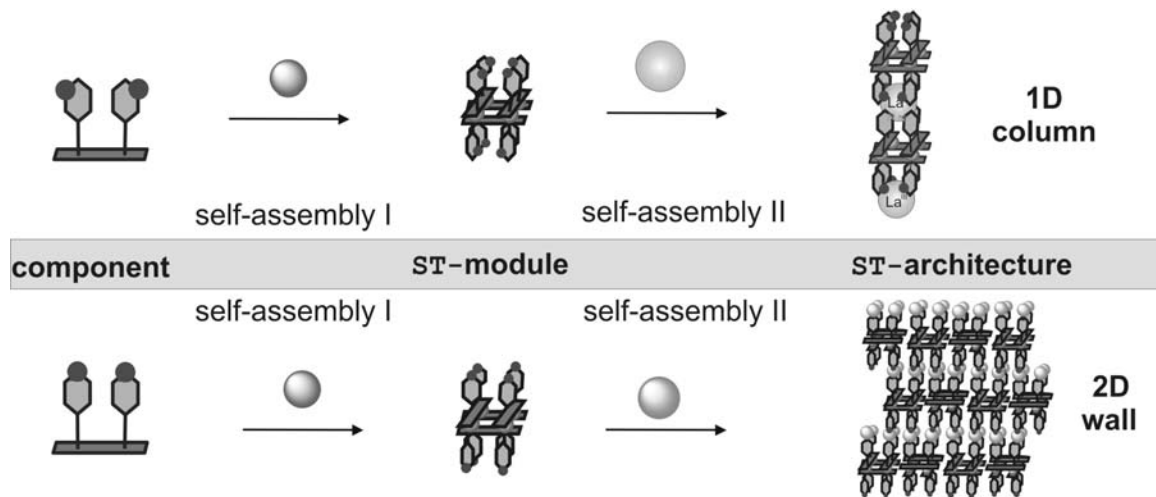


Fig. 16: Two-step hierachical self-assembly of ST-module and of 1D- and 2D-architectures involving different types of metal ions (self-assembly I: Fe^{II} ; self-assembly II: La^{III} or Ag^{I}). [72]

Looking towards more extended structures, the infinite 1D coordination polymer of the composition $[\text{Fe}^{\text{II}}(\text{triazole})_3]_n$ exhibits ST with a well developed hysteresis loop centred around room temperature range.[73] Consequently, this type of compounds was used in first attempts to realize possible applications by the synthesis of thermoreversible magneto-optical gels and the use of this type of polymeric ST-compounds as contrast agents in magnetic resonance imaging techniques. [74] [75] More recent developments were directed towards the incorporation of spin transition centers into extended 3D-metal-organic frameworks.[76] The incorporation of switchable magnetic ST bricks into metal-organic frameworks represents a fascinating approach for new materials with multiple functionalities. Kepert and co-workers reported the successful formation of a cubic nanoporous 3D-network out of ST-[$\text{Fe}^{\text{II}}_2(\text{azpy})_4(\text{NCS})_4$] units ($\text{azpy} = \text{trans-4,4'-azopyridine}$), which can host reversibly guest molecules as ethanol or methanol. While in the absence of absence of the guests, the host-network exhibits no spin transition, the inclusion of alcohol molecules induces spin transition. [77] A second example of 3D molecular solid exhibiting reversible hydration/dehydration induced ST properties in the crystal was reported by Real et. al.. Here, controlled removing and adding of water (by warming or decrease of pressure) leads to reversible shift of the critical temperatures and of the hysteresis width. Obviously, the compounds of the type $[\text{Fe}(\text{pmd})(\text{OH})_2\{\text{M}(\text{CN})_2\}_2]\cdot\text{H}_2\text{O}$ ($\text{pmd} = \text{pyrimidine}$; $\text{M} = \text{Ag}^{\text{I}}$ or Au^{I}) undergo a partially, completely reversible ligand exchange at the ST- Fe^{II} centres, whereby the water molecules can substitute pyrimidine groups.[78]

5 Valence Tautomeric (VT) Compounds

The intramolecular phenomenon called valence tautomerism (VT) involves reversible electron transfer between the d-orbitals of a metal ion and a redoxactive ligand and might be accompanied simultaneously by an intraatomic reorganisation of electron density (spin transition). Valence tautomerism has been reported for complexes containing a variety of metal ions (Mn, [79] Rh, and Ir [80]). However, most of scientific work has been recorded on Co-ions ligated to dioxolene ligands. [81] So far, most of the molecular Co-VT systems involve quinone-type ligands in the dianion form (catecholate, Cat) and in the radical anion form (semiquinone, SQ). The quinone ligand orbitals are generally very close to the metal orbitals and are so able to donate or to accept electrons from the metal. Additionally, most of the VT complexes undergo simultaneous changes in d-orbital occupation as a function of temperature. The LS-Co^{III} form exhibit a the metal electronic configuration $[\pi]^6(\sigma^*)^0$, and the HS-Co^{II} has $[\pi]^5(\sigma^*)^2$, respectively (Figure 17). Occupation of the σ^* orbitals occurs only in the HS-Co^{II} form and results in elongated Co-ligand bond lengths. The transition to longer bond lengths is accompanied by a large entropy increase due to the higher density of vibrational levels in the HS-Co^{II} form.

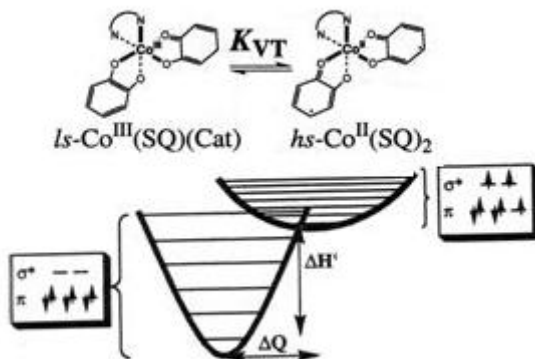


Fig. 17: The schematical representation and electronic configuration of molecular valence tautomerism (from [82])

Subsequently, a complex (N-N)LS-Co^{III}(SQ)(Cat) is transformed into a (N-N)HS-Co^{III}(SQ)₂ complex by increasing the temperature. This significant basically a spin transition and is defined by the low-spin (d^6 Co^{III}) to high-spin (d^7 Co^{II}) multiplicity change at the metal ion. Equally, the electron transfer involves either Co^{III}-reduction or reduction of a SQ to Cat (by Co^{II}).

Most of the VT-complexes reported to date are composed of two dioxolene ligands, a cobalt ion, and a diamine ligand (Figure 17). The most common dioxolene ligands are 3,5-di-*t*-butylsemiquinone (3,5-DBSQ), 3,6-di-*t*-butylsemiquinone (3,6-DBSQ), and their corresponding catecholate forms (3,5-DBCat and 3,6-DBCat).

The magnetic properties of the two tautomeric forms are quite different and are sometimes accompanied of large hysteresis phenomena, as shown in Figure 18. Typical values of χT , the paramagnetic susceptibility product-temperature product, range from 2.4 to 3.8 emu K mol⁻¹ (for the (N-N)HS-Co^{III}(SQ)₂ form) and 0.4 emu K mol⁻¹ for the (N-N)LS-Co^{III}(SQ)(Cat) form. In addition to the magnetic differences, the optical properties of the VT-tautomers differ substantially. Thus, the (N-N)LS-Co^{III}(SQ)(Cat) tautomer is characterized by a band near 16500 cm⁻¹ (ca. 600nm) and a ligand-based intervalence transition near 4000 cm⁻¹ (2500 nm). On the other hand, the (N-N)HS-Co^{III}(SQ)₂ tautomer shows a metsal-to ligand charge transfer (MLCT) band near 13000 cm⁻¹ (770 nm), but no transition in the far-IR region was detected. [83] The interconversion of the two tautomeric forms can be followed quite easily using variable-temperature electronic absorption spectroscopy. The transformation is marked by several isosbestic points, consistent with two species only, i.e. no further intermediates are involved. In addition, it was shown that (N-N)HS-Co^{III}(SQ)₂ can be interconverted reversibly into the (N-N)LS-Co^{III}(SQ)(Cat) tautomer by applying pressure and light. [84] [85]

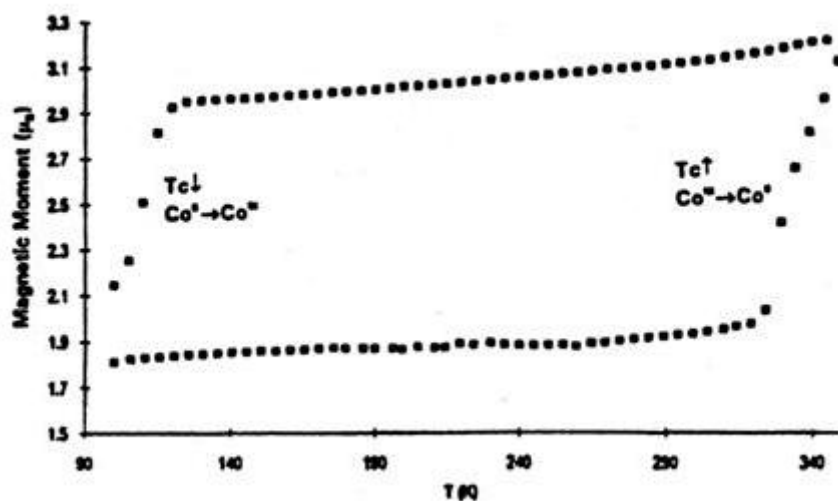


Fig. 18: Magnetisation *vs.* temperature diagram representing the very extended hysteresis loop and magnetic bistability for Co(3,6-DBSQ)₂(PyO). [86]

References

- [1]J.-M. Lehn, Supramolecular Chemistry, Concepts and Perspectives, VCH, Weinheim (1995).
- [2]O. Kahn, *Molecular Magnetism*, VCH, Weinheim (1993).
- [3]I. Fujita, Y. Teki, T. Takui, T. Kinoshita, K. Itoh, F. Miko, Y. Sawaki, H. Iwamura, A. Izuoka, T. Sugawara, J. Am. Chem. Soc. 112, 4074-4075 (1990).
- [4]A. Chiarelli, M. A. Novak, A. Rassat, J. L. Tholence, Nature, 363, 147-149 (1993)
- [5]A. Lappas, K. Prassides, K. Vevekis, D. Arcon, R. Blinc, P. Cevc, A. Amato, R. Feyerherm, F. N. Gygax, A. Schenck, Science 267, 1799-1802 (1995)
- [6]A. J. Banister, A: Bricklebank, I. Lavender, J. M. Rawson, C. I. Gregory, B. K. Tanner, W. Clegg, M. R. J. Elsegood, F. Palacio, Angew. Chem. Int. Ed. 35, 2533-2535 (1996)
- [7]J.J. Girerd, O. Kahn, M. Verdaguer, Inorg. Chem. 19, 274-277 (1980); H. Oshio, U. Nagashima, Inorg. Chem. 31, 3295-3301 (1992)
- [8]S. Decurtins, H. W. Schmalle, H. R. Ostwald, A. Linden, J. Ensling, P. Gütlich, A. Hauser, Inorg. Chim. Acta, 216, 65-73 (1994)
- [9]S. Decurtins, H. W. Schmalle, P. Schneuwly, H. R. Ostwald, Inorg. Chem. 32, 1888-1892 (1993)
- [10]O. Kahn, Adv. Inorg. Chem. 43, 179 (1995)
- [11]O. Kahn, Molecular Magnetism, VCH Weinheim, (1993)
- [12]V. Baron, B. Gillon, J. Sletten, C. Matthoniere, E. Codjovi, O. Kahn, Inorg. Chim. Acta, 235, 69 (1995)
- [13]R. Pellaux, H. W. Schmalle, R. Huber, P. Fischer, T. Hauss, B. Ouliaddiaf, S. Decurtins, Inorg. Chem. 36, 2301-2308 (1997); C. J. Nuttal, P. Day, Chem. Mat. 10, 3050-3057 (1998); E. Coronado, J. Galan-Mascaros, C. Gomez-Garcia, J. Ensling, P. Gütlich, Chem. Eur. J. 6, 552-563 (2000)
- [14]O.Cador, D. Price, J. Larionowa, C. Mathoniere, O. Kahn, J. V. Yakhmi, J. Chem. Mat. 7, 773, (1997)
- [15]M. Pilkington, S. Decurtins, in J. S. Miller, M. Drillon (Eds.) Magnetism: From Molecules to Materials, Vol. 2, Wiley-VCH, Weinheim (2001)
- [16]E. Coronado, J. R. Galan-Mascaros, C. J. Gomez-Garcia, V. Laukhin, Nature 408, 447-449(2000)
- [17]S. Decurtins, H. W. Schmalle, R. Pellaux, P. Schneuwly, A. Hauser, Inorg. Chem. 35, 1451-1460 (1996)
- [18]R. Andres, M. Gruselle, B. Malezieux, M. Verdaguer, J. Vaissermann, Inorg. Chem., 38, 4637-4646 (1999)
- [19]M. Hernandez-Molina, F. Lloret, C. Ruiz, M. Julve, Inorg. Chem. 37, 4031 (1998)
- [20]A.N. Hoden, B. T. Mathias, P. W. Anderson, H. W. Lewis, Phys. Rev. 102, 1463, (1956)
- [21]B.N. Figgis, E.S, Kucharski, M. J. Virtis, J.Am. Chem. S., 115, 176-181 (1993)
- [22]T. Mallah, S. Thebaut, M. Verdaguer, P. Veillet, Science 262, 1554-1557 (1993)
- [23]S. Ferlay, T. Mallah, R. Ouahes, P. Veillet, M. Verdaguer, Nature, 378, 701-703 (1996)]
- [24]J. M. Manriquez, G. T. Yee, R. S. McLean, A. J. Epstein, J. S. Miller, Science, 252, 1415-1417(1991)
- [25]O.Sato, T. Iyoda, A. Fujishima, K. Hashimoto, Science, 272, 704-707(1996)
- [26]a) R. Sessoli, H.-L. Tsai, A. R. Schake, S. Wang, J. B. Vincent, K. Folting, D. Gatteschi, G. Christou, D. N. Hendrickson, J. Am. Chem. Soc.,, 115, 1804-1809, (1993); b) R. Sessoli, D. Gatteschi, A. Caneschi, M. A. Novak, Nature, 365, 141-144, (1993)

- [27]J. R. Friedman, M. P. Sarachik, J. Tejada, R. Ziolo, Phys. Rev. Lett. 76, 3830-3833 (1996)
- [28]W. Wernsdorfer, R. Sessoli, Science, 284, 133-135 (1999)
- [29]A. J. Tasiopoulos, A. Vinslava, W. Wernsdorfer, K. A. Abboud, G. Christou, Angew. Chem. Int. ed. 43, 2117-2121 (2004)
- [30]E. C. Sanudo, W. Wernsdorfer, K. A. Abboud, G. Christou, Inorg. Chem. 43, 4137-4144 (2004); G. Rajaraman, M. Murugesu, E. C. Sanudo, M. Soler, W. Wernsdorfer, M. Heliwell, C. Muryn, J. Raftery, S. J. Teat, G. Christou, E. K. Brechin, J. Am. Chem. Soc. 126, 15445-15457 (2004)
- [31]S. Wang, H.-L. Tsai, K. Folting, W. E. Streib, D. N. Hendrickson, G. Christou, Inorg. Chem. 35, 7578-7589
- [32]W. Wernsdörfer, N. Aliaga-Alcalde, D. N. Hendrickson, G. Christou, Nature, 416, 406-408 (2002)
- [33]S. Hill, R. S. Edwards, N. Aliaga-Alcalde, G. Christou, Science, 302, 1015-1018 (2003)
- [34]W. Wernsdorfer, R. Sessoli, Science, 284, 133-135 (1999)
- [35]A. Cornia, A. C. Faretti, P. Garris, C. Mortalo, D. Bomacchi, D. Matteschi, R. Sessoli, L. Sorace, W. Wernsdorfer, A.-L. Barra, Angew. Chem. Int. Ed. 43, 1136-1139 (2004); H. Oshio, N. Hoshino, T. Ito, J. Am. Chem. Soc. 122, 12602-12603 (2000);
- [36]A. K. Boudalis, B. Donnadieu, V. Nastopoulos, J. M. Clemente-Juan, A. Mari, Y. Sanakis, J.-P. Tuchagues, S. P. Perlepes, Angew. Chem. Int. Ed., 43, 2266-2270 (2004)
- [37]K. Wieghardt, K. Pohl, I. Jibril, G. Huttner, Angew. Chem. Int. Ed. Engl., 23, 77-80 (1984)
- [38]J. C. Goodwin, R. Sessoli, D. Gatteschi, W. Wernsdorfer, A. K. Powell, S. L. Heath, J. Chem. Soc., Dalton Trans., 1835-1840 (2000)
- [39]S. L. Castro, Z. Sun, C. M. Grant, J. C. Bollinger, D. N. Hendrickson, G. Christou, J. Am Soc. Chem., 120, 2365-2375 (1998)
- [40]M. Murrie, S.J. Teat, H. Stoeckli-Evans, H. U. Güdel, Angew. Chem. Int., Ed. 42, 4653-4656 (2003)
- [41]H. Andres, R. Basler, A.J. Blake, C. Cadiou, G Chaboussant, C. M. Grant, H. U. Güdel, M. Murrie, S. Parsons, C. Paulsen, F. Semadini, V. Villar, W. Wernsdörfer, R. E. P. Winpenny, Chem. Eur. J., 8, 4867-4876 (2002)
- [42]J. J. Sokol, A. G. Hee, J. R. Long, J. Am. Chem. Soc., 124, 7656-7657 (2002)
- [43]R. J. Glauber, J. Math. Phys., 4, 294-307 (1963)
- [44]A. Caneschi, D. Gatteschi, n. Lalotti, C. Sangregorio, R. Sessoli, G. Venturi, A. Vindigni. A. Rettori, M. G. Pini, M. A. Novak, Angew. Chem. Int. Ed. 40, 1760-1763 (2001)
- [45]R. Clerac, H. Miysaka, M. Yamashita, C. Coulon, J. Am. Chem. Soc., 124, 12837-12844 (2002)
- [46]R. Lescouezec, J. Vaissermann, C. Ruiz-Perez, F. Lloret, R. Carrasco, M. Julve, M. Verdaguer, Y. Dromzee, D. Gatteschi, W. Wernsdorfer, Angew. Chem. Int. Ed., 42, 1483-1486 (2003)
- [47]A. Caneschi, D. Gatteschi, P. Rey, Inorg. Chem. 30, 3936-3941 (1991)
- [48]S. Mossin, H. Weihe, H. O. Sorensen, N. Lima, R. Sessoli, Dalton Trans., 632-639 (2004)
- [49]K.L. Taft, S. J. Lippard, J. Am. Chem. Soc., 112, 9629-9632 (1990)
- [50]Q. Chen, S. Liu, J. Zubietta, Inorg. Chem., 28, 4434-4437 (1989); N. V. Gerbeleu, Y. T. Struchkow, G. A. Timko, A.S. Batsanov, K. M. Indrichan, G. A. Popowich, Dokl. Acad. Nauk SSSR, 1459 (1990); R. W. Saalfrank, I. Bernt, E. Uller, F. Hampel, Angew. Chem. Int. Ed. , 36, 2482-2485 (1997); I. M. Atkinson, C. Benelli, M. Murrie, S. Parsons, R. E. P. Winpenny, Chem. Comm., 285-286 (1999)

- [51]K. L. Taft, C. D. Delfs, G. C. Papaefthymiou, S. Foner, D. Gatteschi, S. J. Lippard, *J. Am. Chem. Soc.*, 116, 823-831 (1994); A. Cornia, M. Affronte, A.G. M. Jansen, G. L. Abbatì, D. Matteschi, *Angew. Chem. Int. Ed.*, 38, 2264-2267 (1999); O. Waldmann, J. Schühlein, R. Koch, P. Müller, I. Bernt, R.W. Saalfrank, H. P. Andres, H. U. Güdel, P. Allenspach, *Inorg. Chem.*, 28, 5879-5886 (1999); O. Waldmann, R. Koch, S. Schromm, J. Schühlein, P. Müller, I. Bernt, R. W. Saalfrank, F. Hampel, E. Balthes, *Inorg. Chem.*, 40, 2986-2991 (2001)
- [52]A. Caneschi, D. Gatteschi, C. Sangregorio, R. Sessoli, L. Sorace, A. Cornia, M. A. Novak, C. Paulsen, W. Wernsdorfer, *J. Magn. Magn. Mater.*, 200, 182-201 (1999); A. Chiolero, D. Loss, *Phys. Rev. Lett.* 80, 169-172 (1998); M.- H. Julien, Z. H. Jang, F. Borsa, M. Horvatic, A. Caneschi, D. Gatteschi, *Phys. Rev. Lett.*, 83, 227-230 (1999)
- [53]F. Meier, D. Loss, *Phys. Rev. B*; 64, 224411/1-224411/14 (2001)
- [54]O. Waldmann, J. Hassmann, P. Müller, G. S. Hanan, D. Volkmer, U.S. Schubert, J.-M. Lehn, *Phys. Rev. Letters*, 78, 3390-3396 (1997)
- [55]J. van Slageren, R. Sessoli, D. Gatteschi, A. A. Smith, M. Helliwell, R. E. P. Winpenny, A. Cornia, A.-L. Barra, A. G. M. Jansen, E. Rentschler, G. A. Timco, *Chem. Eur. J.*, 8, 277-285 (2002)
- [56]O. Waldmann, J. Hassmann, P. Müller, G. S. Hanan, D. Volkmer, U.S. Schubert, J.-M. Lehn, *Phys. Rev. Letters*, 78, 3390-3396 (1997)
- [57]Y. Shapira, V. Bindilatti, *J. Appl. Phys.* 92, 4155-4160 (2002)
- [58]O. Waldmann, M. Ruben, U. Ziener, P. Müller, J.-M. Lehn, submitted (2004)
- [59]F. K. Larsen, E. J. L. McInnes, H. E. Mkami, J. Overgaard, S. Piligkos, G. Rajaraman, E. Rentschler, A. S. Smith, V. Boote, M. Jennings, G. A. Timco, R. E. P. Winpenny, *Angew. Chem. Int. Ed.*, 42, 1001-1005 (2003); F. K. Larsen, J. Overgaard, S. Parsons, E. Rentschler, G.A. Timco, A. A. Smith, R. E. P. Winpenny, *Angew. Chem. Int. Ed.* , 42, 5978-5981 (2003)
- [60]O. Cador, D. Gatteschi, R. Sessoli, F. K. Larsen, J. Overgaard, A.-L. Barra, S. J. Teat, G. A. Timco, R. E. P. Winpenny, *Angew. Chem. Int. Ed.* 43, 5196-5200 (2004)
- [61]pressure: H. G. Drickamer, *Angew. Chem.* 86, 61-64 (1974); P. Gütlich, Y. Garcia, H. A. Goodwin, *Chem. Soc. Rev.*, 29, 419-427 (2000)
- [62]light: S. Decurtins, P. Gütlich, C. P. Köhler, H. Spiering, A. Hauser, *Chem. Phys. Lett.* 105, 1-9 (1984); S. Decurtins, P. Gütlich, K. M. Hasselbach, H. Spiering, A. Hauser, *Inorg. Chem.* 24, 2174-2180 (1985)
- [63]x-ray: D. Collison, C. D. Garner, C.M. McGrath, J. F. W. Mosselmans, M. D. Roper, J. M. W. Seddon, E. Sinn, N. A. Young, *J. Chem. Soc., Dalton Trans.*, 4371-4376 (1997)
- [64]P. Gütlich, Y. Garcia, H. A. Goodwin, *Chem. Soc. Rev.*, 29, 419-427 (2000)
- [65]P. Gütlich, A. Hauser, H. Spiering, *Angew. Chem. Int. Ed.* 33, 2024-2050 (1994)
- [66]N. Willenbacher, H. Spiering, *J. Phys C: Solid State Phys.* 68, 65-70 (1988)
- [67]J. A. Real, A.B. Gaspar, V. Niel, M. C. Munoz, *Coord. Chem. Rev.*, 236, 121-138 (2003)
- [68]V. Ksenofontov, A. B. Gaspar, J. A. Real, P. Gütlich, *J. Phys. Chem. B*, 105, 12266-12273 (2001); B. A. Leita, B. Moubaraki, K. S. Murray, J. P. Smith, J. D. Cashion, *Chem. Comm.* 156-157, (2004); F. Tunes, M. R. Lees, G. J. Clarkson, M. J. Hannon, *Chem. Eur. J.* 10, 5737-5750 (2004)
- [69]S. Brooker, P. G. Plieger, B. Moubaraki, K. S. Murray, *Angew. Chem. Int. Ed.* 38, 408-410, (1999)
- [70]E. Breuning, M. Ruben, J.-M. Lehn, F. Renz, Y. Garcia, V. Ksenofontov, P. Gütlich, E. Wegelius, K. Rissanen, *Angew. Chem. Int. Ed.*, 39, 2504-2507 (2000); M. Ruben, E. Breuning, J.-M. Lehn, V. Ksenofontov, F. Renz, P. Gütlich, G. Vaughan, *Chem. Eur. J.*, 9, 4422-4429 (2003); M. Ruben, E. Breuning, J.-M. Lehn, V. Ksenofontov, P. Gütlich,

- G. Vaughan, J. Mag. Mat., 272-276, e715-e717 (2004)
- [71]A. B. Gaspar, V. Ksenofontov, J. A. Real, P. Gütlich, Chem. Phys. Lett., 373, 385-391 (2003)
- [72]M. Ruben, U. Ziener, J.-M. Lehn, V. Ksenofontov, P. Gütlich, G. B. M. Vaughan, Chemistry, 11, 94-100 (2005)
- [73]J. Kröber, E. Codjovi, O. Kahn, F. Groliere, C. Jay, J. Am. Chem. Soc., 115, 9810-9811 (1993)
- [74]O. Ribeau, A. Colin, V. Schmitt, R. Clerac, Angew. Chem. Int. Ed. 43, 3283-3286 (2004)
- [75]R. N. Muller, L. Vander Elst, S. Laurent, J. Am. Chem. Soc., 125, 8405-8407 (2003)
- [76]J. A. Real, E. Andres, M. C. Munoz, M. Julve, T. Granier, A. Bousseksou, F. Varret, Science, 268, 265-267 (1995)
- [77]G.J. Halder, C. J. Kepert, B. Moubaraki, K.S. Murray, J. D. Cashion, Science, 298, 1762-1765 (2002)
- [78]V. Niel, A. L. Thompson, M. C. Munoz, A Galet, A. E. Goeta, J. A. Real, Angew. Chem. Int. Ed. 42, 3760-3763 (2003)
- [79]a) A. Caneschi, A. Dei, Angew. Chem. Inter. Ed. 37, 3005-3007, (1998); b) A. S. Attia, C. G. Pierpont, Inorg. Chem 34, 1172, (1995); A. S. Attia, C. G. Pierpont, Inorg. Chem 36, 6184, (1997); A. S. Attia, C. G. Pierpont, Inorg. Chem 37, 3051, (1998)
- [80]C. W. Lange, M. Földeaki, V. I. Nevodchikov, G. A. Abakumov, C. G. Pierpont, J. Am. Chem. Soc., 114, 4220-4227 (1992); G.A. Abakumov, G. A. Razvuaev, V. I. Nevochikov, V. K. Cherkasov, J. Organomet. Chem., 341, 485 (1988)
- [81]C. G. Pierpont, C. W. Lange, Prog. Inorg. Chem. 41, 331, (1994); C. G. Pierpont, R. M. Buchanan, Coord. Chem Rev, 38, 45 (1981); W. Kaim, Coord. Chem. Rev. 76, 187 (1987) and references herein.
- [82]D. G. Shultz in J. S. Miller, M. Drillon (Eds.) Magnetism: From Molecules to Materials, Vol. 2, Wiley-VCH, Weinheim (2001)
- [83]D. M. Adams, L. Noddleman, D. N. Hendrickson, Inorg. Chem., 36, 3966 (1997)
- [84]C. Roux, D. M. Adams, J. P. Itie, A. Polian, D. N. Hendrickson, M. Verdaguer, Inorg. Chem., 35, 2846, (1996)
- [85]D. M. Adams, B. Li, J. D. Simon, D. N. Hendrickson, Angew. Chem. Int. Ed., 34, 1481 (1995)
- [86]O.-S Jung, D. H. Jo, Y.-L. Lee, B. J. Chonklin, C. G. Pierpont, Inorg. Chem. 37, 19 (1997)